Estimating a mean transport velocity in the marginal ice zone using ice-ocean prediction systems

Graig Sutherland[1], Victor Aguiar[2,3], Lars-Robert Hole[2], Jean Rabault[4,5], Mohammed Dabboor[1], and Øyvind Breivik[2,6]

[1]Environmental Numerical Prediction Research, Environment and Climate Change Canada, Dorval, QC, Canada
[2]Norwegian Meteorological Institute, Bergen, Norway
[3]Department of Physics and Technology, The Arctic University of Norway, Tromsø, Norway
[4]Norwegian Meteorological Institute, Oslo, Norway
[5]Department of Mathematics, University of Oslo, Oslo, Norway
[6]Geophysical Institute, University of Bergen, Bergen, Norway

Correspondence: Graig Sutherland (graigory.sutherland@ec.gc.ca)

Abstract. Understanding the transport of objects and material in the marginal ice zone (MIZ) is critical for human operations in polar regions. This can be the transport of pollutants, such as spilled oil, or the transport of objects, such as drifting ships and search and rescue operations. For emergency response, the use of environmental prediction systems are required, which predict ice and ocean parameters and are run operationally by many centres in the world. As these prediction systems predict both ice and ocean velocities, as well as ice concentration, it must be chosen how to combine this data to best predict the mean transport velocities. In this paper we develop the idea of a mean transport velocity, which combines both ice and ocean velocities in the MIZ and weights them by ice concentration. We combine this with the traditional leeway model, which is used in oil spill and search and rescue modelling, and allow for different leeway coefficients in both the ocean and ice and weight them by ice concentration. Using drifting buoys from a dedicated experiment in the MIZ, optimal leeway coefficients are determined for ice and ocean velocities from two operational prediction systems. The results using the two prediction systems are similar and give leeway values of 3% of the wind for the ocean leeway and 2% and 30° to the right of the wind for the ice leeway. This mean transport model is compared with traditional transport models and the distance error after 48 hours lead time can be reduced by a factor of 2.

1 Introduction

Estimating the transport of objects and material in the marginal ice zone (MIZ) is a crucial aspect of polar operations. This can
be related to search and rescue operations (Rabatel et al., 2018) as well as the transport of oil and other contaminants (French-McCay et al., 2017; Nordam et al., 2019). The requirement of accurate transport estimates for these processes is exacerbated
by the remoteness of these regions. Thus, accurate predictions up to at least 48 hours, are required to provide sufficient time
to coordinate response efforts. Due to the numerous transient processes in the ocean, these short-term predictions can be
particularly difficult to predict accurately (Christensen et al., 2018).

The first step in predicting transport in the MIZ are accurate predictions of ice, water and wind velocities, and in the
Arctic there are a few products which provide forecast data of at least 48 hours. A couple examples of such Arctic systems
being the Regional Ice-Ocen Prediction System (RIOPS) in Canada (Dupont et al., 2015) and the TOPAZ system as part
of the Copernicus Marine Environment Monitoring Service (CMEMS) (Sakov et al., 2012). These prediction systems will
predominantly have the ocean and ice components coupled, and in general do not include forcing from surface waves. Rarely
they are coupled with the atmosphere, but one example of an ice-ocean-atmosphere coupled model is the Canadian Arctic
Prediction System (CAPS) which is the RIOPS system two-way coupled with the GEM (Global Environmental Multi-scale)
atmospheric model (Côté et al., 1998b, a; Girard et al., 2014). The ice models used in these prediction systems assume a
continuous ice cover and a viscous-plastic rheology, which is typically derived from principles introduced by Hibler III (1979).
For ice concentrations of less than 80%, the ice is assumed to be in "free drift" as the rheology is expected to have a minimal
impact on the dynamics (Hibler III, 1979). While free drift models exist, and they perform quite well when compared with
observations, they do require data in order to tune the drag coefficients (Schweiger and Zhang, 2015) which can be difficult to
obtain in the Arctic.

It is common for the short-term prediction of drifting objects to include a leeway term, which is a fraction of the wind that is
added to the predicted water velocity. This has been common for a long time in search and rescue (Breivik et al., 2011) and oil
spill trajectory modelling (Spaulding, 2017). These leeway values can represent direct wind forcing on the object (Kirwan Jr
et al., 1975), and/or wind-dependent physics which are not included in the ice-ocean prediction system. As most ice-ocean
prediction systems do not include surface waves it is common to include the Stokes drift (Breivik and Christensen, 2020)
which can be approximated by a leeway coefficient (Breivik et al., 2011; Sutherland et al., 2020). In addition, material at the
surface, such as oil but also ice, will strongly attenuate surface waves creating an additional force on the material (Weber,
2001). Oil and ice also impact the "roughness" of the surface; slicks in the case of oil which reduce the roughness (Wu, 1983),
and the presence of form drag in the MIZ which can increase roughness (Lüpkes et al., 2012; Tsamados et al., 2014). For oil, it
has long been established that the competing wind and wave effects combine for a net leeway of about 3% of the velocity (Wu,
1983). For sea ice it is not clear whether a leeway term should be included in the drift, however, ice-ocean prediction systems
such as CAPS and TOPAZ do not explicitly include processes associated with surface waves or form drag due to the ice
roughness. Therefore, a non-zero leeway term in the MIZ may be necessary.

There are only a few examples of using a leeway coefficient with the drift of sea ice, and these are typically restricted to cases where there are no ocean current measurements available and the ice speed is modelled as solely a function of the wind. Wilkinson and Wadhams (2003) observed an ice leeway which was dependent on ice concentration. The leeway values ranged from 3.9% for ice concentrations less than 25% to 2.2% for ice concentrations greater than 75%. More recently, Lund et al. (2018) observed that the wind and sea ice motion is not always well correlated and that ice leeway coefficients span a large range of values from 3.5 to 5% across a wide range of ice concentrations in the Arctic MIZ. In these papers, it is possible that some of the ice motion was due to tidal and/or inertial motions, which will not directly scale with the instantaneous wind and would lead to uncertainties in the above estimates.

While typically leeway coefficients are determined for particular objects using detailed field measurements (Breivik et al., 2011), recently it was shown by Sutherland et al. (2020) that leeway coefficients can also be predicted using environmental prediction systems. The mean leeway coefficients using the model data input were found to be consistent with detailed observations and independent of the choice of environmental prediction system. However, these principles have only been applied in open ocean conditions and have not been tested in the presence of sea ice. It would seem that there are certain analogues with the open ocean that would warrant the use of a leeway coefficient in the MIZ. First, most ice-ocean prediction systems don't include surface waves, which are not uncommon to the MIZ and will impact the drift (Weber, 1987; Squire, 2020). In addition, in the MIZ where ice concentrations are typically less than 80%, the ice is said to be in free drift and the ice motion will depend strongly on a accurate parameterization of the drag coefficient (Cole et al., 2017) and less sensitive to the internal ice stress (Hibler III, 1979). Form drag due to sea ice is also another physical process which will effect the ice motion and has a strong effect in the MIZ (Lüpkes et al., 2012).

In this paper we test a leeway model for the general transport of material and objects in the MIZ using ice-ocean prediction systems used to support operational activities and observations from four ice drifters specifically deployed at various ice concentrations in the MIZ. The outline of the paper is as follows. The general leeway model for the MIZ is described in Section 2. Section 3 describes the data, the ice-ocean prediction systems and the methodology used in calculating and testing the leeway coefficients. Results are presented in section 4 followed by the conclusions.

2 Transport equations for the MIZ

Ice and ocean surface velocities in the MIZ are strongly coupled. In the dynamical models of ice-ocean prediction systems, this is through the relative friction between the ocean and ice components. Most ice-ocean prediction systems will have the ice and ocean components two-way coupled. Differences between ice and ocean surface velocities can arise due to ice inertia, which is generally negligible in the MIZ, and internal stresses within the ice, which are also negligible for ice concentrations less than 80% (Hibler III, 1979). So the ice and ocean surface velocities in the MIZ are predominantly in a steady-state free drift mode, with the magnitude, as predicted by ice-ocean prediction systems, being dependent on the drag coefficients and the ice concentration.

Given the uncertainties associated with modelling velocities in the MIZ, it makes sense to use both ice and ocean velocities to derive a general transport velocity. This is precisely the approach used for oil spill modelling in ice-covered waters (Nordam et al., 2019), where a mean transport velocity is calculated and the ice and surface ocean components are weighted by a function of ice concentration. The model used by the oil spill community uses some empirical estimates for the weighting function as well as for the leeway. We will use this idea of a mean transport model as a template, but will make it more general for a wider use. First, we will go through the oil transport equations and then develop a more general model for transport in the MIZ.

2.1 Oil transport equation in the MIZ

The basic equation for the advection velocity in ice-covered water used by the oil spill community (Nordam et al., 2019) is

$$\mathbf{u}_o = k_i \mathbf{u}_i + (1 - k_i)(\mathbf{u}_w + \alpha_w \mathbf{U}_{10}),\tag{1}$$

where $\mathbf{u}_o$ is the oil velocity, $\mathbf{u}_w$ is the water velocity, $\mathbf{u}_i$ is the ice velocity, $\mathbf{U}_{10}$ is the wind velocity at 10 m, α_w is a leeway coefficient for oil in water which is typically about 3% (Spaulding, 2017; Nordam et al., 2019) and k_i is the ice transfer coefficient and a function of ice concentration A. Often k_i is presented as a piece-wise linear function of ice concentration (Nordam et al., 2019), commonly referred to as the "80/30" rule, and defined as

$$k_i^{80/30} = \begin{cases} 0 & \text{if } A < 0.3, \\ \frac{A - 0.3}{0.5} & \text{if } 0.3 \leq A < 0.8, \\ 1 & \text{if } 0.8 \leq A. \end{cases}\tag{2}$$

The arguments for the "80/30" rule originated from observations by Venkatesh et al. (1990) and are qualitative in nature. Venkatesh et al. (1990) observed that for sea ice concentrations greater than 80% the oil appeared to drift with the surrounding ice. For ice concentrations less than 30%, the oil drifted with the water. In between these two limits a linear weighting is assumed. The functional form of (2) has not been investigated in detail (French-McCay et al., 2017; Nordam et al., 2019), but any form for k_i will inevitably be a monotonically increasing function of ice concentration with the limits $k_i = 0$ when $A = 0$ (no ice) and $k_i = 1$ when $A = 1$ (all ice).

2.2 General transport equation in the MIZ

For the transport of objects and material in the MIZ we propose a more general equation than (1) that allows for a non-zero leeway coefficient in the ice,

$$\mathbf{u}_o = k_i (\mathbf{u}_i + \alpha_i \mathbf{U}_{10}) + (1 - k_i)(\mathbf{u}_w + \alpha_w \mathbf{U}_{10}),\tag{3}$$

where α_i is the leeway coefficient in the ice. As mentioned previously, k_i in (3) can be any monotonically increasing function of ice concentration A that has the limits $k_i = 0$ at $A = 0$ and $k_i = 1$ at $A = 1$. The simplest parameterization of k_i that satisfies these conditions is the linear relation $k_i = A$ and this will be used for this study.

The inclusion of a leeway coefficient in the sea ice has certain analogues with the open ocean. First, most ice-ocean prediction systems don't include surface waves, which are not uncommon to the MIZ and will impact the drift (Weber, 1987; Squire, 2020). There are also advantages to using both the ice and ocean components for transport. One potential advantage is that the wind stress in coupled ice-ocean prediction systems (Sakov et al., 2012; Dupont et al., 2015), as well as for wave models (Masson and LeBlond, 1989; Rogers et al., 2016; Liu et al., 2020), is partitioned as a linear function of ice concentration and, therefore, biases in the ice concentration could lead to biases in the ice and ocean velocities. Using a weighted mean ice-ocean velocity ensures that all of the wind-generated currents will be present and biases can be adjusted via the leeway coefficient. Essentially, the assumption is that we will formulate a transport model which assumes that a weighted average of the ice and ocean velocities in the MIZ, along with a corresponding leeway coefficient to be determined, will provide a more accurate estimate for transport velocities than using either the ocean or the ice velocities separately. This is similar to how third generation wave models solve the wave action equation in the MIZ, that is they weight the source terms by ice concentration and calculate one mean wave spectrum for both the ice and water components combined.

3   Data and Methodology

3.1   Ice Drifters

Four ice drifters, designed to measure wave-ice interactions (Rabault et al., 2020), were deployed on various ice floes in the MIZ approximately 250 km north of Svalbard on 19 September 2018. The initial location for each drifter was chosen to sample a broad range of ice conditions ranging from solitary floes (approximately 10% ice coverage) to more densely packed sea ice (approximately 90% ice coverage) in a transect perpendicular to the ice edge (Figure 1). The ice floes were relatively flat with no visible signs of ridging and an estimated thickness between 50 to 75 cm. The diameters for each was estimated to be 10-15 m for the lowest ice concentration and 20-25 m for the next two higher concentration floes. For the ice floe in the highest ice concentration it was difficult to estimate the floe diameter due to the compactness.

The drifters are equipped with an inertial motion unit to measure the directional wave spectra and a GPS sensor which provides accurate measurements of the geographic location and time. The data are recorded on each drifter and sent via Iridium approximately every 3 hours. The drifter velocities were calculated using the forward difference in geographic locations.

The drifters transmitted data from 19 September 2018. Two drifters survived until 1 October 2018 (14435 and 14437) while the other two (14432 and 14438) stopped reporting at approximately 26 September 2018. From the available data it appears that each of the drifters stopped transmitting when they had left the MIZ (Figure 1).

3.2   Ice-ocean prediction systems

The Canadian Arctic Prediction System (CAPS) is a coupled atmosphere-ice-ocean prediction system, with separate analyses for the atmosphere, ice and ocean components, and a 48 hour forecast is run four times a day at Environment and Climate Change Canada (ECCC) as part of the Year of Polar Prediction. The ice-ocean component is a 1/12° coupled NEMO-CICE
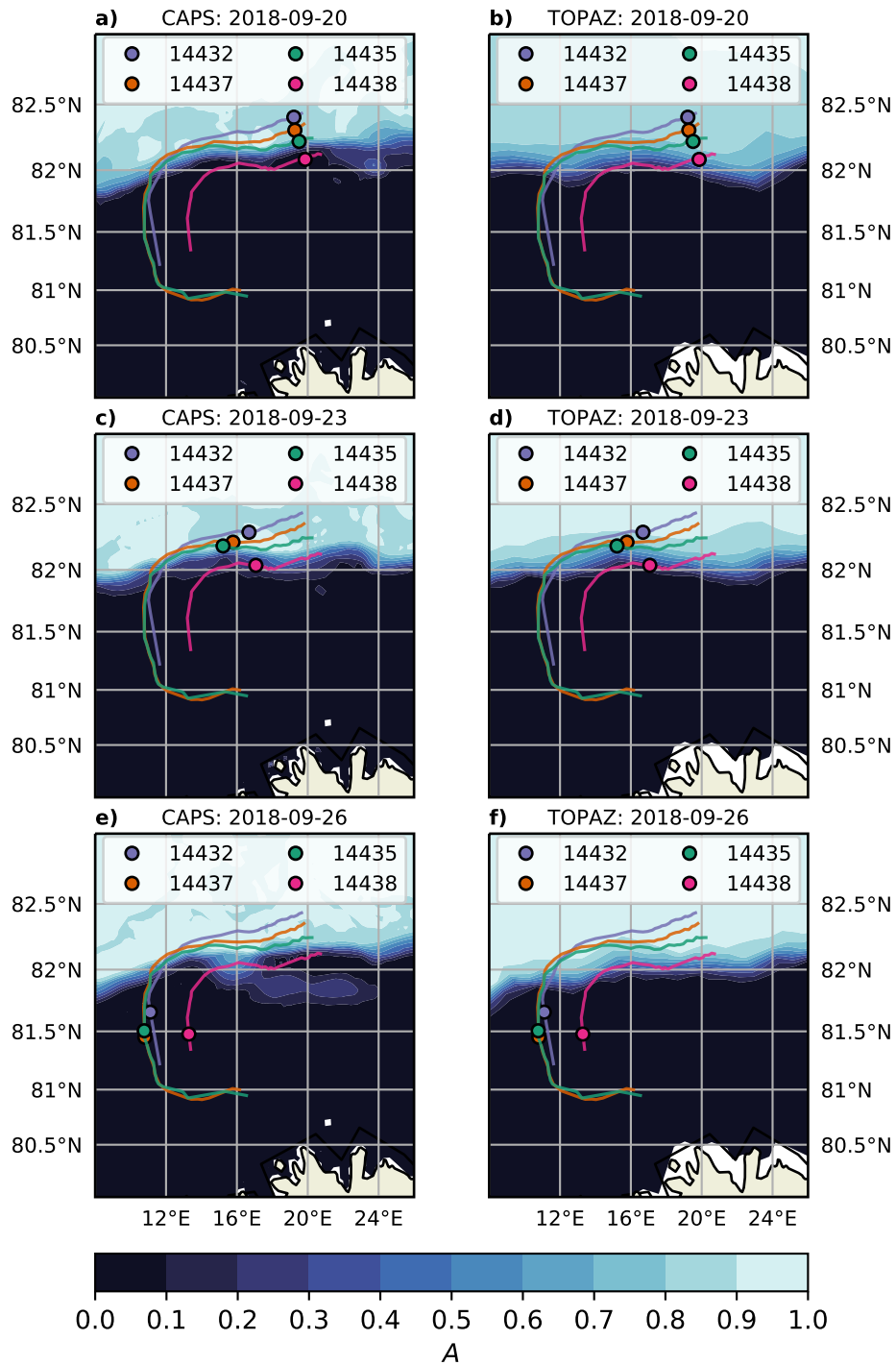
Figure 1. Drifter tracks (-) and locations (o) at three different times during their respective trajectories. Filled contours of ice concentration are shown as calculated by CAPS (a, c, e), and TOPAZ (b, d, f). Drifter IDs, from furthest in the ice to nearest to ocean, are 14432 (blue), 14437 (orange), 14435 (green) and 14438 (red). Drifters exit the MIZ at approximately 2018-09-25 00:00 UTC.

configuration as in Dupont et al. (2015). The ice-ocean component is coupled with an atmospheric model on a higher (3 km) grid. The dynamical core of the atmospheric component of CAPS is GEM (Global Environmental Multiscale), a non-hydrostatic model which solves the fully compressible Euler equations (Côté et al., 1998b, a; Girard et al., 2014).

TOPAZ is a coupled ice-ocean data assimilation system covering the North Atlantic and Arctic oceans (Sakov et al.,
145   2012). TOPAZ represents the Arctic component of the Copernicus Marine Environment Monitoring Service (CMEMS) system (marine.copernicus.eu). Atmospheric forcing is provided by the European Centre for Medium-Range Weather Forecasting (ECMWF). The ocean component of TOPAZ is the HYbrid COordinate Model (HYCOM), which is a hybrid model consisting of z-level vertical coordinates in the upper (mixed) layer and isopycnal coordinates below. The horizontal resolution is 12.5 km on a polar stereographic projection. The ocean model is coupled with a single thickness category ice model with
150   elastic-viscous-plastic (EVP) rheology. Details can be found in Sakov et al. (2012) and Xie et al. (2017).

For all simulations, the wind forcing from CAPS is used. The CAPS model has a grid resolution of roughly 3 km, includes data assimilation, and is freely available. TOPAZ is forced by ECMWF IFS forecast data which has a spatial resolution of $0.1°$ ($\simeq 9$ km) on a regular lat/lon grid (https://resources.marine.copernicus.eu/documents/PUM/CMEMS-ARC-PUM-002-ALL.pdf). The choice of using only one of the wind forcing data sets is partially motivated by the ECMWF IFS forecast data
155   requiring a license, but also allows for a simpler analysis to focus on the ice-ocean systems.

Snapshots of the ice concentration field (Figure 1) as well as the along-track time series of ice concentration (Figure 2) are calculated for both CAPS and TOPAZ. A consistent feature between the two ice concentrations is that after approximately 25 September 2018 both CAPS and TOPAZ predict that there is no ice at the drifter locations. This will allow us to test the model of (3) for an object that travels between ice and open water. There are also clearly some differences between the predicted ice
160   concentrations, which are most likely due to the different assimilation cycles of each model. While the analysis of the ice field in CAPS is updated for each forecast (every 12 hours) the TOPAZ fields have a weekly analysis cycle, which could lead to the differences, especially for the two drifters which begin in lower ice concentrations (drifters 14435 and 14438).

A comparison of the model and observed velocities for each drifter is shown in Figure 3. Time series for ice, water and wind (2%) velocities, interpolated in time and space to available drifter observations, are shown. It is apparent from Figure 3 that
165   the observed drifter velocities are nearly always greater than either of the ice and water velocities from CAPS or TOPAZ. Ice and ocean velocities in CAPS vary in magnitude and direction more than those from TOPAZ. This is most likely due to ocean tides being included in CAPS, while these are not in TOPAZ, as this region is known to have large diurnal tidal currents due to a near-resonant, forced topographic wave propagating around the Yermak Plateau (Hunkins, 1986; Padman et al., 1992).

3.3   Calculating leeway coefficients

170   As the drifters were deployed on ice floes, it is assumed that the drift of these ice floes in the MIZ can be given by (3). Ice drifters have been previously used by French-McCay et al. (2017); Babaei and Watson (2020) in comparing transport equations with the drift of ice floes. However, even for ice floes over a wide range of ice concentrations, the weighting of (3) states that the ice floe will drift more like the water in low ice concentrations and more like the ice in high ice concentrations. The primary assumption for using the ice floes as a proxy for general transport is that the ice floe is small enough that inertial forces are
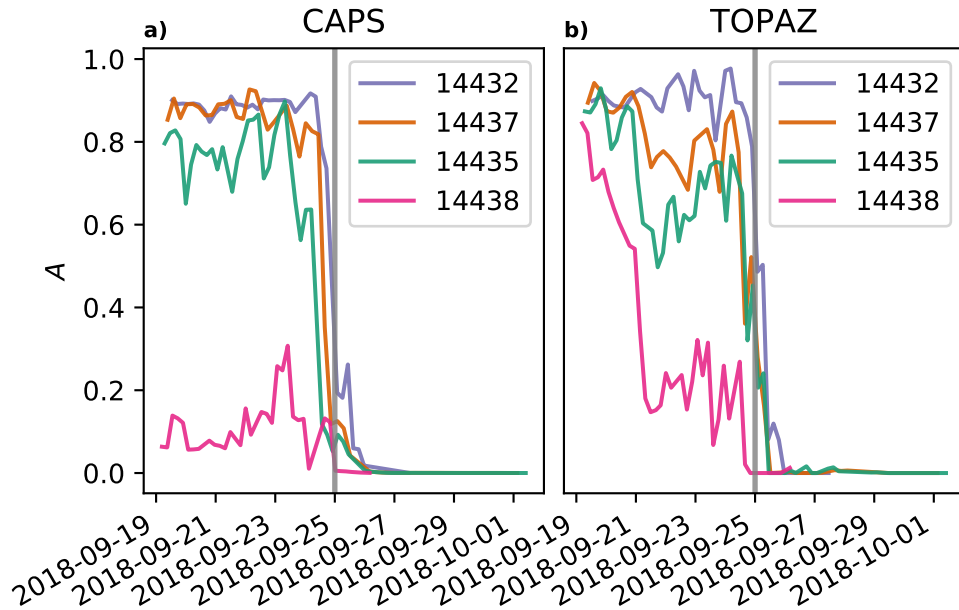
Figure 2. Ice concentration interpolated to drifter tracks as calculated by a) CAPS and b) TOPAZ. The vertical grey line shows the approximate time (2018-09-25 00:00 UTC) that the drifters leave the MIZ.

negligible. To investigate this assumption, the results from using (3) will be compared with results using (1) as well as an ocean-leeway model ($k_i = 0$, $\alpha_w = 0.03$) and an ice-only model ($k_i = 1$, $\alpha_i = 0$).

The optimal leeway coefficients to be used in (3) are determined by minimizing the mean absolute error (MAE) between the observed and predicted velocities. The leeway coefficients are assumed to be constant in time, and are a vector with both a downwind and crosswind component. It is also important to assess the sensitivity to these leeway coefficients, which is not trivial as the calculated MAE is a function of four variables as each α_i and α_w are vectors. To look at the sensitivity, 2-D slices are made through the 4-D MAE field to show the relative sensitivity for α_i for a fixed α_w and vice versa for α_w for a fixed α_i. The fixed points for these 2-D slices are selected from averaging the optimal leeway values for all the drifters and ice-ocean prediction systems.

4 Results and Discussion

4.1 Ice and water leeway coefficients

The MAE between the observed drifter velocity and the model velocity from (3) is minimized for each drifter and choice of ice-ocean prediction system. The optimal leeway coefficients, as well as the MAE in km/day, are located in Table 1 for using the CAPS forcing and Table 2 for the TOPAZ forcing. To demonstrate the relative sensitivity to the choice of leeway coefficients,
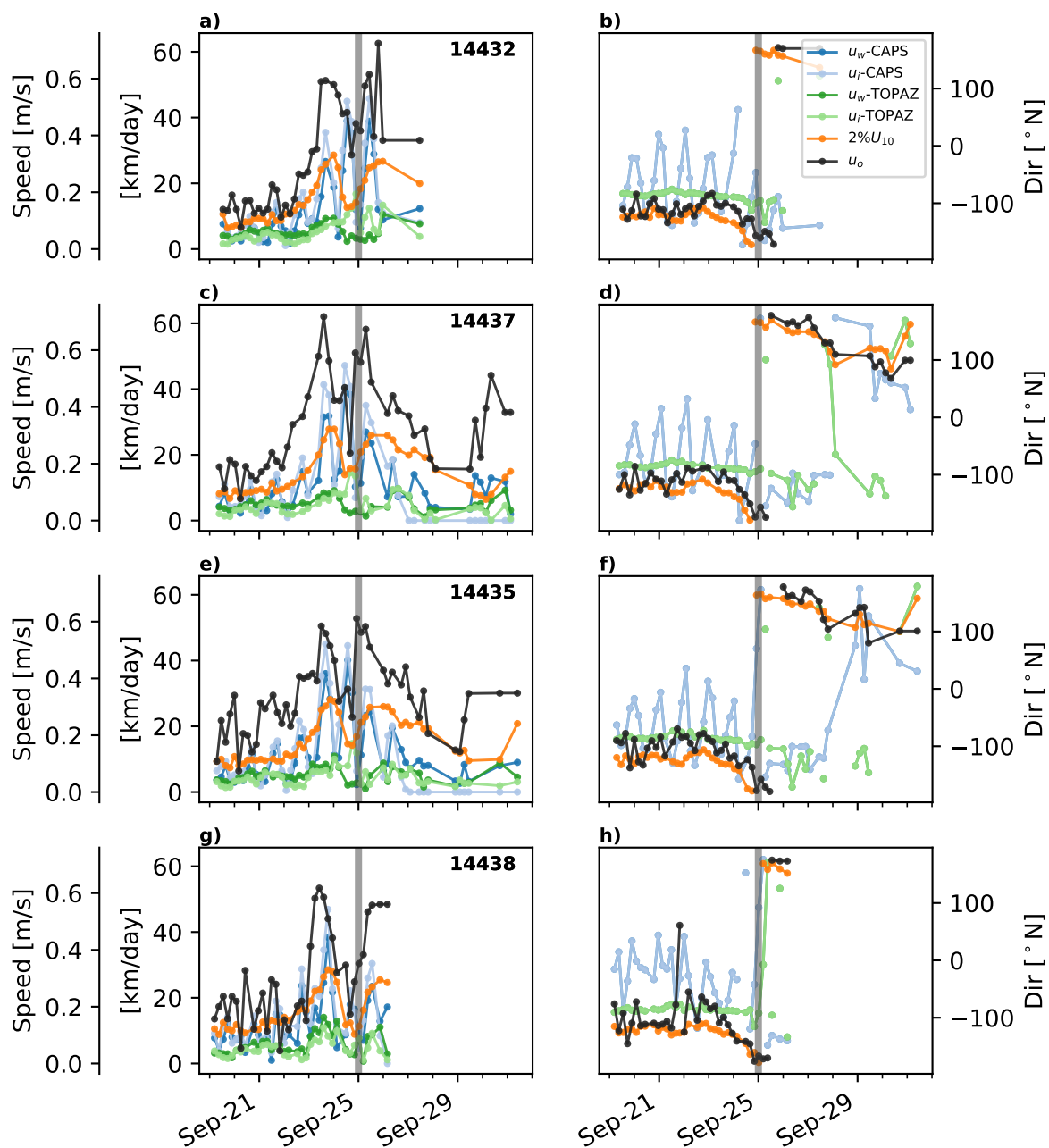
Figure 3. Magnitude and direction of observed drifter velocities ($\mathbf{u}_o$, black) and predicted wind velocity ($2\%\mathbf{U}_{10}$, orange) ice ($\mathbf{u}_i$) and water velocities ($\mathbf{u}_w$) from CAPS (blue) and TOPAZ (green) interpolated to the drifter locations. The strong diurnal tidal current is clearly observed in CAPS, but is absent from TOPAZ as this model does not include tides. The vertical grey line shows the approximate time when the drifters exit the MIZ.

Table 1. Best fit for leeway coefficients using the CAPS forcing. MAE* is the mean absolute error using leeway values of $\alpha_i = 0.02e^{-i\pi/6}$ and $\alpha_w = 0.03$. Negative angles imply clockwise direction relative to wind.

Drifter	$|\alpha_i|$	Ang(α_i)	$|\alpha_w|$	Ang(α_w)	MAE (km/day)	MAE* (km/day)
14432	1.7%	-30°	2.3%	-5°	9.4	10.0
14437	2.1%	-25°	2.9%	5°	11.3	11.4
14435	2.4%	-35°	2.5%	5°	11.9	12.3
14438	2.8%	-45°	2.7%	5°	13.4	13.5

Table 2. Best fit for leeway coefficients using the TOPAZ forcing. MAE* is the mean absolute error using leeway values of $\alpha_i = 0.02e^{-i\pi/6}$ and Ang(α_i) and $\alpha_w 0.03$. Negative angles imply clockwise direction relative to wind.

Drifter	$|\alpha_i|$	Ang(α_i)	$|\alpha_w|$	Ang(α_w)	MAE (km/day)	MAE* (km/day)
14432	2.9%	-25°	3.3%	-30°	9.8	12.3
14437	3.2%	-25°	2.8%	-5°	11.8	13.0
14435	3.4%	-30°	2.7%	-10°	10.6	12.1
14438	1.5%	-5°	2.9%	-15°	11.5	12.2

2-D slices of the MAE contours are made through a fixed leeway coefficient. That is, the downwind and crosswind contours for the ice leeway are presented for a fixed water leeway and vice versa. Optimal leeway values are found to be approximately $\alpha_w = 0.03$ and $\alpha_i = 0.02e^{-i\pi/6}$ and these are used for the constant leeway coefficients used for the MAE slices. No leeway angle is used for α_w, but for α_i an angle of -30° is found where the negative implies clockwise rotation relative to the wind as we are using complex notation for our vectors. The MAE for these fixed leeway coefficients are also shown in Tables 1 and 2, denoted MAE* in each Table, and the difference is less than 1.5 km/day for each. Although not shown here, the MAE contours are qualitatively similar for different choices of fixed leeway coefficients with the primary difference being in the magnitude of the MAE.

Filled contours of MAE for α_i, with $\alpha_w = 0.03$, for the downwind and crosswind components are shown in Figure 4. The MAE contours for each drifter are very similar when using the CAPS data or the TOPAZ data. There is a clear sensitivity related to the ice concentration as the drifter furthest in the ice (14432) has the sharpest contour gradients in MAE and the drifter at the ice edge (14438) shows very little change in MAE for different values of α_i. Not including drifter 14438, the optimal value for α_i is approximately 0.02 and 30° to the right of the wind using the CAPS data and 0.03 and 30° to the right of the wind using the TOPAZ data. The difference between 0.02 and 0.03 are within the 1 km/day MAE contour, which is less than 10% of the total MAE.

Filled contours of MAE for α_w, with $\alpha_i = 0.02e^{-i\pi/6}$, for the downwind and crosswind components are shown in Figure 5. Not surprisingly, the MAE contours in Figure 5 have the opposite sensitivity as those in Figure 4, with sharper contour gradients
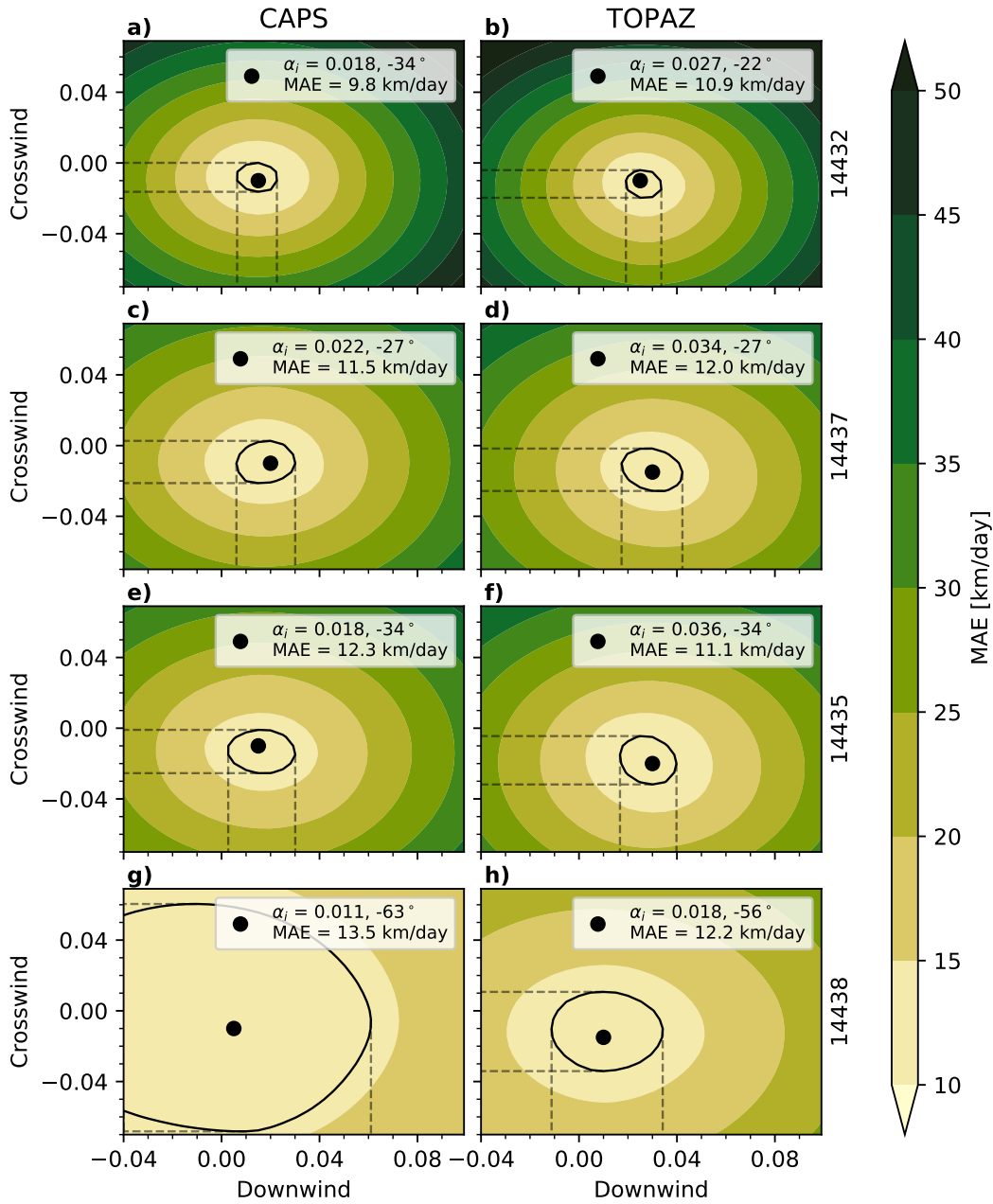
Figure 4. Filled contours of MAE (in km/day) between observed drift velocities and (3) for the along and cross-wind components of α_i with $\alpha_w = 0.03$. The left column uses the CAPS forcing and the right column uses TOPAZ forcing. The black dot shows the location of the MAE minimum and the black contour line shows the MAE value within 1 km/day of the minimum. Each row is for an individual drifter in order from high ice concentration at the top to low ice concentration at the bottom. Sensitivity to to the choice of α_i is much greater in the high ice concentration than the low.
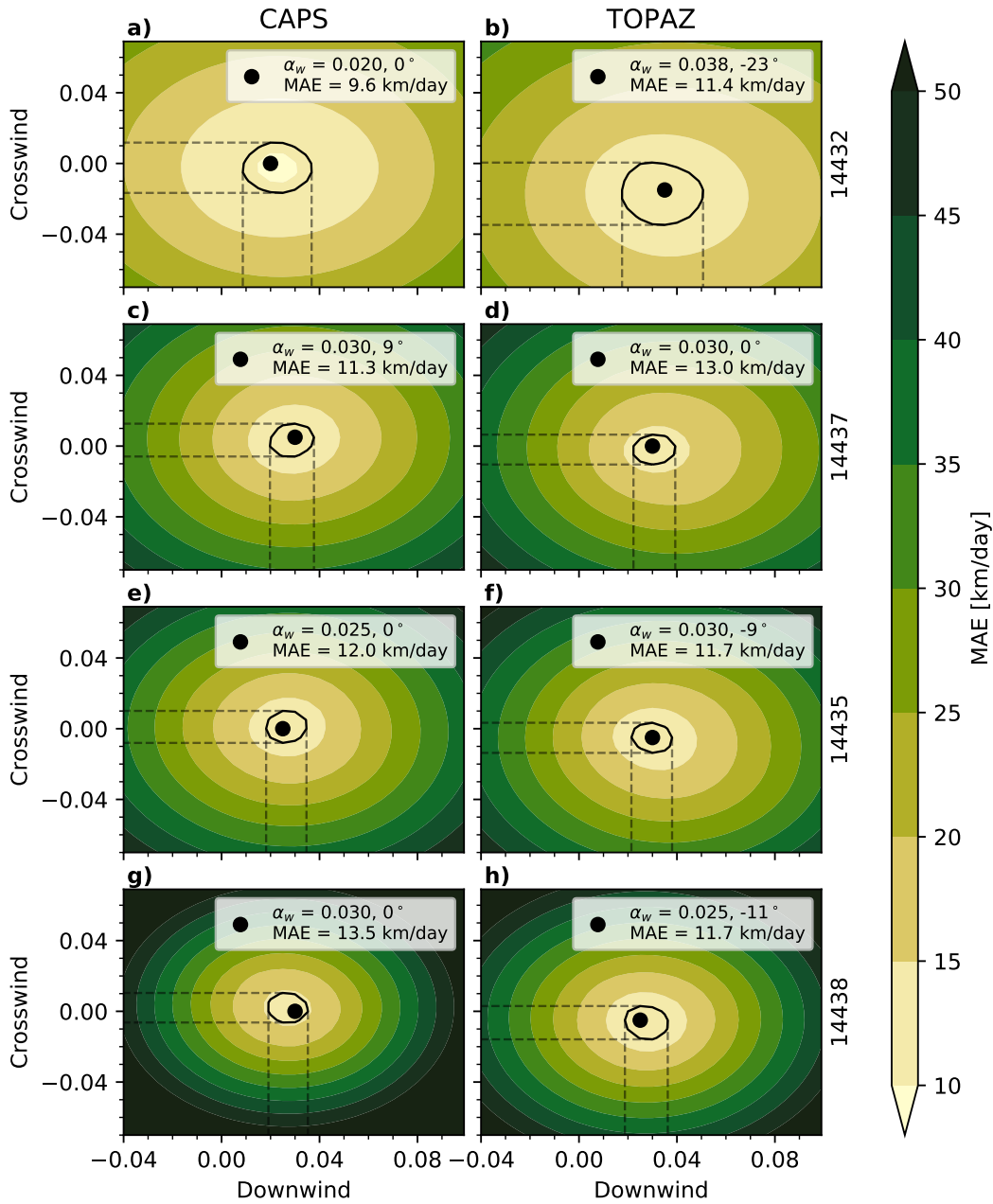
Figure 5. Filled contours of MAE (in km/day) between observed drift velocities and (3) for the along and cross-wind components of α_w with $\alpha_i = 0.02e^{-i\pi/6}$. The left column uses CAPS forcing and the right column uses TOPAZ forcing. The black dot shows the location of the MAE minimum and the black contour line shows the MAE value within 1 km/day of the minimum. Each row is for an individual drifter in order from high ice concentration at the top to low ice concentration at the bottom. Sensitivity to choice of α_w is opposite to that of α_i in Figure 4 with less sensitivity in high ice concentration relative to low.

Table 3. Mean and standard deviation of separation distance, d, after 48 hours (in km) from Figure 7 for each drifter, forcing, and drift model.

drift	14432		14437		14435		14438	
model	CAPS	TOPAZ	CAPS	TOPAZ	CAPS	TOPAZ	CAPS	TOPAZ
linear	9.4 ± 5.5	18.2 ± 8.9	6.2 ± 2.4	15.0 ± 7.0	9.5 ± 2.5	14.4 ± 6.9	8.9 ± 6.6	10.1 ± 7.0
80/30	27.7 ± 14.6	30.4 ± 17.9	28.4 ± 14.1	30.6 ± 11.7	18.6 ± 8.0	25.4 ± 5.1	8.6 ± 6.8	9.7 ± 7.3
ice	31.8 ± 13.5	32.6 ± 18.9	37.1 ± 9.8	39.0 ± 15.9	35.0 ± 5.4	38.6 ± 10.7	22.5 ± 15.6	22.8 ± 17.2
ocean	15.0 ± 6.3	20.2 ± 12.5	10.5 ± 3.8	18.0 ± 9.2	12.5 ± 3.2	19.0 ± 5.5	8.6 ± 6.8	$10.1 \pm 7.$

in MAE for the lowest ice concentration and MAE showing minimal sensitivity to the choice of α_w in high ice concentration. Also, similar to Figure 4, the MAE values in Figure 5 are similar in magnitude when using either CAPS or TOPAZ data and range between 10 and 14 km/day.

4.2 Short-term trajectory predictions

Lagrangian trajectories are simulated with MLDPn (Modèle Lagrangien de Dispersion de Particules d'ordre n), a Lagrangian dispersion model developed at ECCC (D'Amours et al., 2015) adapted for aquatic use (Paquin et al., 2020). Virtual trajectories are launched every 12 hours along the observed trajectory, between 20 September to 25 September 2018. Two different drift models are used for the simulations. First, the classic drift equation given by (1) with $k_i^{80/30}$ and leeway coefficients $\alpha_w = 0.03$ and $\alpha_i = 0$. These leeway coefficients are chosen for the 80/30 method as they are typical values used in the MIZ (Nordam et al., 2019). Second, the more general (3) with the linear transfer function $k_i = A$ and $\alpha_w = 0.03$ and $\alpha_i = 0.02 e^{-i\pi/6}$. For comparison, we test an ice-only transport ($k_i = 1$, $\alpha_i = 0$) and ocean-only transport ($k_i = 0$, $\alpha_w = 0.03$). The use of a leeway in the ocean is for consistency with 1).

A few examples of the observed and modelled trajectories for each drifter can be found in Figure 6. A more detailed presentation of the separation distance, d, after 48 hours between the observed and modelled trajectories as a function of trajectory start time is located in Figure 7. A summary of the mean and standard deviation of the separation distance d can be found in Table 3).

For the drifter furthest in the ice, 14432, and the drifter second furthest in the ice, 14437, the separation distance after 48 hours is the smallest for forecasts beginning before 21 September and this does not vary much with choice of transport model or ice-ocean forcing (Figure 7a,b). This changes rapidly after 21 September where the predicted trajectories using the 80/30 and ice-only transport models perform poorly (large separation distance), while the linear model and ocean-leeway models do not produce such a dramatic change (Figure 7a,b). The time when the transport models diverge corresponds with the increase in wind speed (Figure 3a). As the ice-only and 80/30 transport models do not have a leeway term (these two transport models are identical for $A > 0.8$), that the leeway term can improve 48 hour trajectories when using ice-ocean prediction systems.

Drifter 14435, which is in an intermediate ice concentration, has a slightly different response than the previous two drifters in higher ice concentration. Similar to the other drifters, the leeway models (ocean-leeway, linear) have smaller trajectory
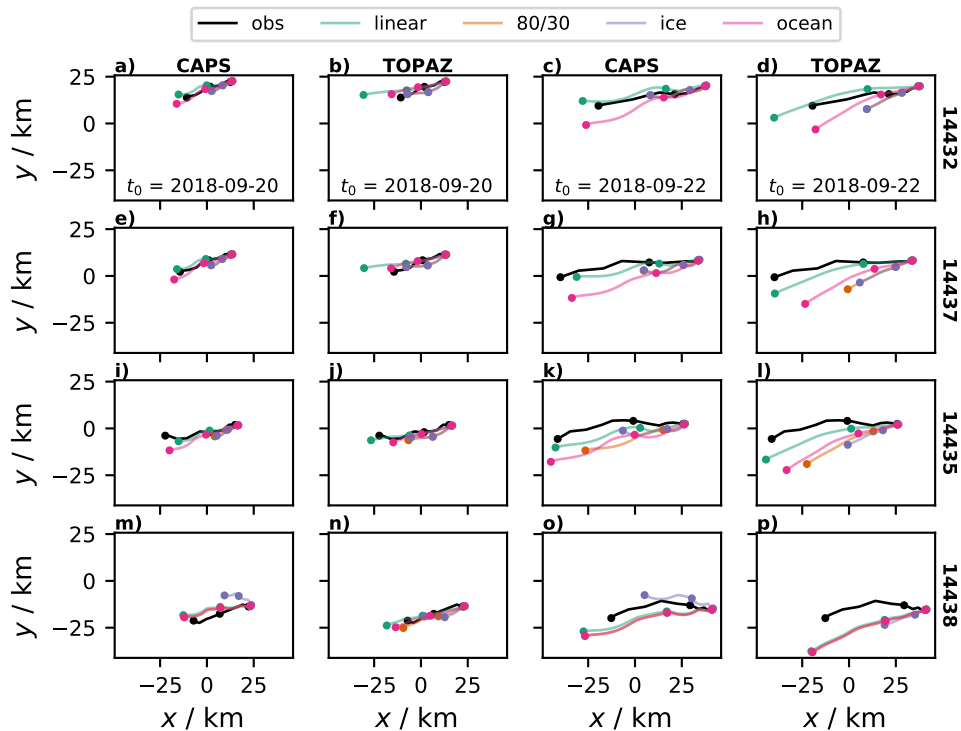
Figure 6. Examples of observed and modelled 48 hour trajectories. Each column corresponds to a combination of unique starting time and choice of ice-ocean forcing. Each row corresponds to a unique drifter. The dots represent locations at 24 hour intervals. The x and y axis are in km and the choice of origin is arbitrary. The different predicted tracks are linear using (3), 80/30 using (1), ice which uses only the ice velocities, and ocean which uses the ocean velocities plus 3% leeway.

errors than the non-leeway models (ice-only, 80/30 for $A > 0.8$). Where drifter 14435 is different is that the intermediate ice concentrations associated with this drifter trajectory, approximately 60-80%, create two distributions where the separation distances are sometimes similar to the ice-only model (Figure 7e, before 21 September) and where the distributions are more similar to those of the ocean-leeway (Figure 7e, after 21 September).

235   For the drifter in the lowest ice concentration, 14438, the 80/30, linear, and ocean-leeway models all have essentially the same trajectory error. As the ice concentration, as provided by the model, are less than 0.3 (with the exception of TOPAZ before 21 September) it is expected that these three transport models should reproduce the same trajectory.

    In general, the linear model using the best-fit leeway coefficients produces the smallest separation distance as well as the least amount of variation as a function of simulation start time (Table 3). The ice-only transport model had the largest tra-
240 jectory errors even though we are using drifters on ice floes as our proxy for transport in the MIZ. The ocean-leeway had errors comparable to the linear model and the 80/30 model did not perform well in high ice concentration but did perform well in low ice concentration. These results were generally independent of the choice of CAPS or TOPAZ for the
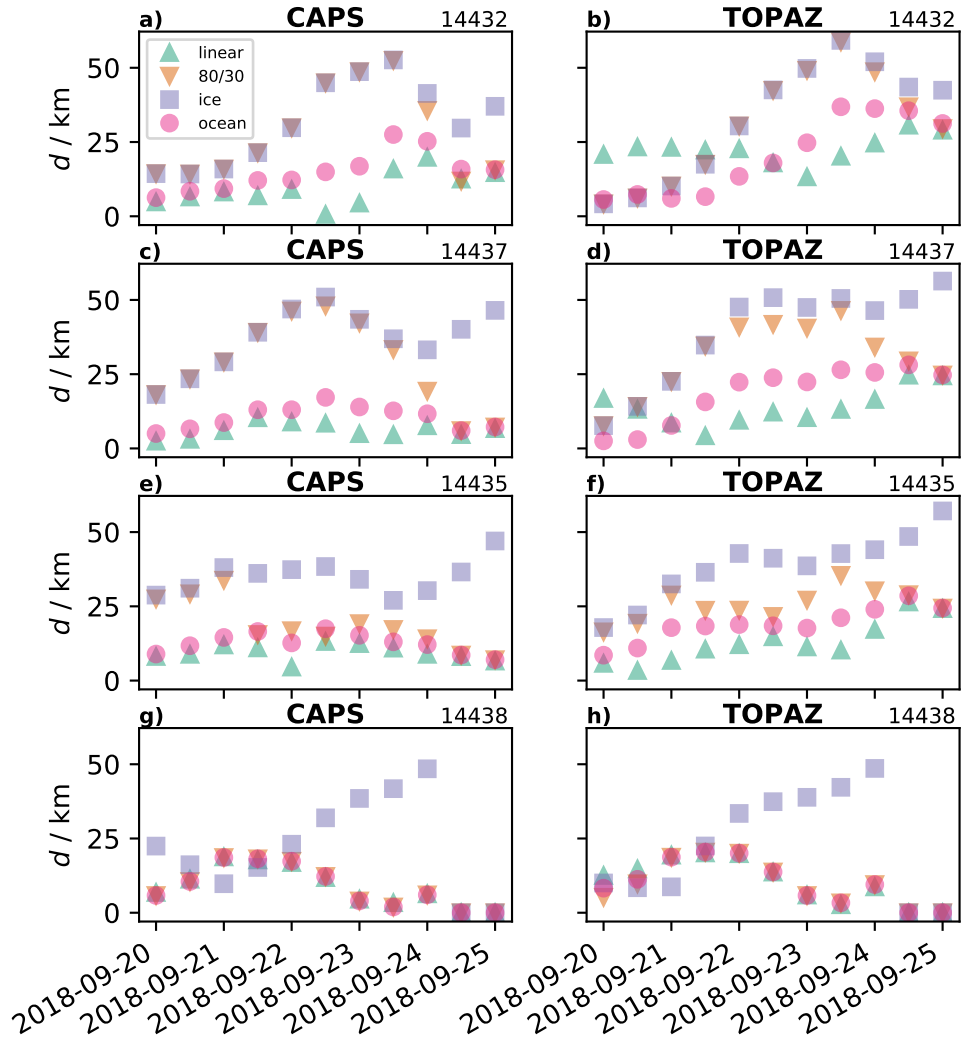
Figure 7. Drifter separation, d in km, after 48 hours. The horizontal axis denotes the start times for each simulation simulation so that d is measured at 48 hours after the time shown on the axis. The linear model corresponds to (3), the 80/30 model to (1), ice corresponds to the prediction with just ice velocities with no leeway and ocean corresponds to the prediction with just ocean velocities plus 3% leeway. The solid horizontal lines show the mean separation distance for each respective drift model. The inclusion of a leeway coefficient does reduce separation distance between observed and predicted trajectories with the linear weighted model providing the best results.

ice-ocean forcing. It would be interesting to expand the analysis to other ice-ocean prediction systems, for example GOFS 3.1(https://www7320.nrlssc.navy.mil/GLBhycomcice1-12/), but this is beyond the scope of the current paper and is left to future research.

5 Conclusions

Presented here is a general equation to improve the transport of objects and material in waters with a mix of ice and ocean using ice-ocean prediction systems. The equation is a generalized leeway model and assumes a linear weighting of the ice and ocean velocities based on ice concentration and allows for a non-zero leeway, which can vary in both magnitude and direction, in both the ice and ocean components. Optimal leeway coefficients are calculated by minimizing the error between available observed drifter velocities in the MIZ and the model velocities calculated using ice-ocean velocities provided by two different coupled ice-ocean prediction systems: CAPS and TOPAZ. This general leeway model is inspired by the leeway model used for oil transport in ice-covered waters (Nordam et al., 2019), but we allow for a non-zero ice leeway to account for missing physics and uncertainties in the ice model.

By minimizing the error between the available observed and modelled trajectories, optimal values for the water and ice leeway coefficients, α_w and α_i respectively, were determined. Optimal values for α_w were found in the range $0.02 < \alpha_w < 0.04$ and for α_i they were $0.01 < \alpha_i < 0.03$ with a mean direction of $30°$ to the right of the wind. Slightly larger values for α_i using the TOPAZ data compared to the CAPS data. For α_w, this range of values is consistent with 3% required for the prediction of surface drifters (Sutherland et al., 2020) and oil spill modelling (Nordam et al., 2019). The α_i values are curiously consistent with canonical values used for icebergs of about 2% of the wind and $30°$ to the right (Leppäranta, 2011).

To assess the quality of the general leeway model we compared the trajectory difference between several transport models for a series of short-term (48 hour) forecasts using the two different ice-ocean prediction systems (CAPS and TOPAZ). The general leeway model with the linear $k_i = A$ is used with the optimal leeway values of $\alpha_w = 0.03$ and $\alpha_i = 0.02$ and $30°$ to the right of the wind direction. This is compared with the 80/30 transport equation used by the oil spill community, as well as an ice-only transport ($k_i = 1$, $\alpha_i = 0$) as well as an ocean-leeway model ($k_i = 0$, $\alpha_w = 0.03$). Results did not vary greatly between the two ice-ocean forcings. The linear general leeway model consistently had the smallest trajectory error for all four of the drifters. Somewhat surprisingly the ocean-leeway model consistently had the second smallest errors, even for the drifter in the highest ice concentration (14432). This is most likely due to the ice-ocean prediction systems being coupled so that the respective velocities will be strongly correlated in the MIZ when the internal ice stresses are small. The inclusion of the leeway is also key as it will compensate for missing physics, notably from surface waves which are not included in the ice-ocean prediction systems, and can as well compensate for any biases in the respective drag coefficients in the atmosphere-ice-ocean system. The 80/30 model had mixed results and generally had smaller prediction errors for smaller ice concentrations than for large. This is most likely due to the lack of a leeway coefficient in the ice. The ice-only prediction had the largest errors, further emphasizing the importance of a leeway coefficient for accurate short-term prediction of drift in the MIZ.

275 It is not obvious why the errors associated with calculating the leeway coefficients are similar between the CAPS and TOPAZ forcing (Figures 4 and 5, while the separation errors are much smaller for CAPS than TOPAZ (Figure 7). One likely explanation is due to the drifter observations being available every 3 hours, hence velocities calculated using forward differences are also every 3 hours, while CAPS and TOPAZ provide currents every hour. While averaging the CAPS and TOPAZ forcing would most likely reduce the magnitude of the MAE, it is not expected that this averaging would affect the relative sensitivity, i.e. the

280 optimal leeway coefficients should not change. As CAPS includes tides, and therefore has more variability at these frequencies than TOPAZ (Figure 3), impacts on the magnitude of the MAE will probably be greater for CAPS than TOPAZ. However, simulation of the trajectories don't require the observed drifter velocities and should therefore be more accurate, i.e. the results in Figure 7 and summarized in Table 3.

It is clear that from the available data that the inclusion of an ice leeway improves short-term predictions in the MIZ.

285 However, there is not enough information to ascertain whether this is due to missing physics in the prediction systems or correcting for biases that are correlated with the wind. More data would be welcome and dedicated experiments which provide high resolution (sub-daily) observations are excellent for investigating short-term dynamics in the MIZ. Data sources, such as the International Arctic Buoy Program (IABP) (https://iabp.apl.uw.edu) could be another source of data for drift in the MIZ, but as these buoys are deployed in the pack ice they are dependent on the sea ice dynamics to reach the MIZ, provided they

290 survive the journey, as well as other data data products to determine whether they are in the MIZ or not. Attempting to use IABP could prove useful for understanding short-term dynamics, but given the unknowns mentioned above it is beyond the scope of this paper.

The likely physical explanation for including a leeway in the ice is due to surface waves, which are not uncommon in the MIZ (Rabault et al., 2020). The waves effect the motion of sea ice in two ways: first, there is an additional Lagrangian drift

295 due to the presence of waves (the Stokes drift), as well as an additional force due to the attenuation of the surface waves, often called the radiation stress (Weber, 1987). This force will be in the direction of wave propagation, so since the waves are generally entering the ice from the ocean ocean that this can cause the ice edge to compact (Sutherland and Dumont, 2018). There are also large uncertainties associated with the drag coefficients (Heorton et al., 2019) that could also be part of the leeway coefficient. It should also be emphasized that while the use of an ice leeway improved predictions in the MIZ, there is

300 little reason to expect that this would be the case in the pack ice where internal stresses significantly impact the drift. In such a case, a more sophisticated expression for α_i, which depends on ice concentration such that $\alpha_i \to 0$ as $A \to 1$ would most likely be required that also preserves some of the improvements shown in the MIZ.

Data availability. The drifter data can be accessed at https://thredds.met.no/thredds/catalog/metusers/jeanr/data_papers/drift_barents_2018/
catalog.html?dataset=metusers/jeanr/data_papers/drift_barents_2018/drift_data.nc. TOPAZ forecasts are available on the Copernicus Marine

305 Enrivonment Monitoring Service FTP server (https://resources.marine.copernicus.eu) at nrt.cmems-du.eu/Core/ARCTIC_ANALYSIS_FORE
CAST_PHYS_002_001_a/dataset-topaz4-arc-myoceanv2-be/. CAPS ice-ocean forecasts are available at http://dd.alpha.meteo.gc.ca/yopp/
model_riops/ and the atmospheric forecasts at http://dd.alpha.meteo.gc.ca/yopp/model_caps/.

Author contributions. This article was written by GS with input from all co-authors. GS conceived of the idea, with feedback from all co-authors, and wrote the software for data analysis and production of figures. VA, LH and MD contributed to preliminary data analysis. JR designed the drifters and was responsible for data collection and quality control. JR, LH and ØB contributed to drifter deployment.

Competing interests. No competing interests are present.

Acknowledgements. GS and MD thank the Ocean Protection Plan (OPP) for funding and support of this work. JR, VA, LRH and ØB thank the Nansen Legacy (Arven etter Nansen) project for contributing to the development and deployment of the wave loggers. JR thanks the Norwegian Research Council under the PETROMAKS2 scheme (project DOFI, grant number 28062) for funding. LRH and VA would also like to thank the Fram Centre MIKON Flagship program for support through the OSMICO project. Our warmest thanks go to the crew of the R/V Kronprins Haakon, for the time spent on the boat during the cruise and their help in deploying the drifters.

References

Babaei, H. and Watson, D.: A preliminary computational surface oil spill trajectory model for ice-covered waters and its validation with two oil spill events: A field experiment in the Barents Sea and an accidental spill in the Gulf of Finland, Marine Pollution Bulletin, 161, 111 786, 2020.

Breivik, Ø. and Christensen, K. H.: A combined Stokes drift profile under swell and wind sea, J. Phys. Oceanogr., 50, 2819–2833, 2020.

Breivik, Ø., Allen, A. A., Maisondieu, C., and Roth, J. C.: Wind-induced drift of objects at sea: The leeway method, Appl. Ocean Res., 33, 100–109, 2011.

Christensen, K. H., Breivik, Ø., Dagestad, K.-F., Röhrs, J., and Ward, B.: Short-Term Predictions of oceanic drift, Oceanography, 31, 59–67, 2018.

Cole, S. T., Toole, J. M., Lele, R., Timmermans, M.-L., Gallaher, S. G., Stanton, T. P., Shaw, W. J., Hwang, B., Maksym, T., Wilkinson, J. P., et al.: Ice and ocean velocity in the Arctic marginal ice zone: Ice roughness and momentum transfer, Elementa: Science of the Anthropocene, 5, 2017.

Côté, J., Desmarais, J.-G., Gravel, S., Méthot, A., Patoine, A., Roch, M., and Staniforth, A.: The operational CMC–MRB global environmental multiscale (GEM) model. Part II: Results, Mon. Wea. Rev., 126, 1397–1418, 1998a.

Côté, J., Gravel, S., Méthot, A., Patoine, A., Roch, M., and Staniforth, A.: The operational CMC–MRB global environmental multiscale (GEM) model. Part I: Design considerations and formulation, Mon. Wea. Rev., 126, 1373–1395, 1998b.

D'Amours, R., Malo, A., Flesch, T., Wilson, J., Gauthier, J.-P., and Servranckx, R.: The Canadian Meteorological Centre's atmospheric transport and dispersion modelling suite, Atmosphere-Ocean, 53, 176–199, 2015.

Dupont, F., Higginson, S., Bourdallé-Badie, R., Lu, Y., Roy, F., Smith, G., Lemieux, J.-F., Garric, G., and Davidson, F.: A high-resolution ocean and sea-ice modelling system for the Arctic and North Atlantic oceans, Geosci. Mod. Dev., 8, 1577–1594, 2015.

French-McCay, D. P., Tajalli-Bakhsh, T., Jayko, K., Spaulding, M. L., and Li, Z.: Validation of oil spill transport and fate modeling in Arctic ice, Arctic Science, 4, 71–97, 2017.

Girard, C., Plante, A., Desgagné, M., McTaggart-Cowan, R., Côté, J., Charron, M., Gravel, S., Lee, V., Patoine, A., Qaddouri, A., et al.: Staggered vertical discretization of the Canadian Environmental Multiscale (GEM) model using a coordinate of the log-hydrostatic-pressure type, Mon. Wea. Rev., 142, 1183–1196, 2014.

Heorton, H. D., Tsamados, M., Cole, S., Ferreira, A. M., Berbellini, A., Fox, M., and Armitage, T. W.: Retrieving sea ice drag coefficients and turning angles from in situ and satellite observations using an inverse modeling framework, J. Geophys. Res. Oceans, 124, 6388–6413, 2019.

Hibler III, W.: A dynamic thermodynamic sea ice model, J. Phys. Oceanogr., 9, 815–846, 1979.

Hunkins, K.: Anomalous diurnal tidal currents on the Yermak Plateau, J. Mar. Res., 44, 51–69, 1986.

Kirwan Jr, A., McNally, G., Chang, M., and Molinari, R.: The effect of wind and surface currents on drifters, J. Phys. Oceanogr., 5, 361–368, 1975.

Leppäranta, M.: The drift of sea ice, Springer Science & Business Media, 2011.

Liu, Q., Rogers, W. E., Babanin, A., Li, J., and Guan, C.: Spectral modeling of ice-induced wave decay, Journal of Physical Oceanography, 50, 1583–1604, 2020.

Lund, B., Graber, H. C., Persson, P., Smith, M., Doble, M., Thomson, J., and Wadhams, P.: Arctic sea ice drift measured by shipboard marine radar, J. Geophys. Res. Oceans, 123, 4298–4321, 2018.

Lüpkes, C., Gryanik, V. M., Hartmann, J., and Andreas, E. L.: A parametrization, based on sea ice morphology, of the neutral atmospheric
355   drag coefficients for weather prediction and climate models, Journal of Geophysical Research: Atmospheres, 117, 2012.

Masson, D. and LeBlond, P.: Spectral evolution of wind-generated surface gravity waves in a dispersed ice field, J. Fluid Mech., 202, 43–81,
    1989.

Nordam, T., Beegle-Krause, C., Skancke, J., Nepstad, R., and Reed, M.: Improving oil spill trajectory modelling in the Arctic, Mar. Pollut.
    Bull., 140, 65–74, 2019.

360 Padman, L., Plueddemann, A. J., Muench, R. D., and Pinkel, R.: Diurnal tides near the Yermak Plateau, J. Geophys. Res. Oceans, 97,
    12 639–12 652, 1992.

Paquin, J.-P., Lu, Y., Taylor, S., Blanken, H., Marcotte, G., Hu, X., Zhai, L., Higginson, S., Nudds, S., Chanut, J., et al.: High-resolution
    modelling of a coastal harbour in the presence of strong tides and significant river runoff, Ocean Dynamics, 70, 365–385, 2020.

Rabatel, M., Rampal, P., Carrassi, A., Bertino, L., and Jones, C. K.: Impact of rheology on probabilistic forecasts of sea ice trajectories:
365   application for search and rescue operations in the Arctic, The Cryosphere, 12, 935–953, 2018.

Rabault, J., Sutherland, G., Gundersen, O., Jensen, A., Marchenko, A., and Breivik, Ø.: An open source, versatile, affordable waves in ice
    instrument for scientific measurements in the Polar Regions, Cold Reg. Sci. Technol., 170, 102 955, 2020.

Rogers, W. E., Thomson, J., Shen, H. H., Doble, M. J., Wadhams, P., and Cheng, S.: Dissipation of wind waves by pancake and frazil ice in
    the autumn Beaufort Sea, J. Geophys. Res. Oceans, 121, 7991–8007, 2016.

370 Sakov, P., Counillon, F., Bertino, L., Lisæter, K., Oke, P., and Korablev, A.: TOPAZ4: an ocean-sea ice data assimilation system for the North
    Atlantic and Arctic, Ocean Sci., 8, 633–656, 2012.

Schweiger, A. J. and Zhang, J.: Accuracy of short-term sea ice drift forecasts using a coupled ice-ocean model, Journal of Geophysical
    Research: Oceans, 120, 7827–7841, 2015.

Spaulding, M. L.: State of the art review and future directions in oil spill modeling, Mar. Pollut. Bull., 115, 7–19, 2017.

375 Squire, V. A.: Ocean wave interactions with sea ice: a reappraisal, Annual Review of Fluid Mechanics, 52, 37–60, 2020.

Sutherland, G., Soontiens, N., Davidson, F., Smith, G. C., Bernier, N., Blanken, H., Schillinger, D., Marcotte, G., Rø"hrs, J., Dagestad,
    K.-F., Christensen, K. H., and Breivik, Ø.: Evaluating the Leeway Coefficient of Ocean Drifters Using Operational Marine Enviornmental
    Prediction Systems, J. Atmos. Oceanic Technol., 37, 1943–1954, 2020.

Sutherland, P. and Dumont, D.: Marginal ice zone thickness and extent due to wave radiation stress, J. Phys. Oceanogr., 48, 1885–1901,
380   2018.

Tsamados, M., Feltham, D. L., Schroeder, D., Flocco, D., Farrell, S. L., Kurtz, N., Laxon, S. W., and Bacon, S.: Impact of variable atmospheric
    and oceanic form drag on simulations of Arctic sea ice, J. Phys. Oceanogr., 44, 1329–1353, 2014.

Venkatesh, S., ElTahan, H., Comfort, G., and Abdelnour, R.: Modelling the behavior of oil spills in ice-infested waters, Atmosphere-Ocean,
    28, 303–329, 1990.

385 Weber, J. E.: Wave attenuation and wave drift in the marginal ice zone, J. Phys. Oceanogr., 17, 2351–2361, 1987.

Weber, J. E.: Virtual wave stress and mean drift in spatially damped surface waves, J. Geophys. Res. Oceans, 106, 11 653–11 657, 2001.

Wilkinson, J. and Wadhams, P.: A salt flux model for salinity change through ice production in the Greenland Sea, and its relationship to
    winter convection, J. Geophys. Res. Oceans, 108, 2003.

Wu, J.: Sea-surface drift currents induced by wind and waves, J. Phys. Oceanogr., 13, 1441–1451, 1983.

390 Xie, J., Bertino, L., Counillon, F., Lisæter, K. A., and Sakov, P.: Quality assessment of the TOPAZ4 reanalysis in the Arctic over the period
    1991-2013., Ocean Sci., 13, 2017.